Toxicology in Vitro 40 (2017) 134–143

Contents lists available at ScienceDirect

Toxicology in Vitro

journal homepage: www.elsevier.com/locate/toxinvit

Toxicological interactions of silver nanoparticles and non-essential metals in human hepatocarcinoma cell line

Renata Rank Miranda [a,*], Arandi Ginane Bezerra Jr [b], Ciro Alberto Oliveira Ribeiro [a], Marco Antônio Ferreira Randi [a], Carmen Lúcia Voigt [c], Lilian Skytte [d], Kaare Lund Rasmussen [d], Frank Kjeldsen [e], Francisco Filipak Neto [a,*,1]

[a] Departamento de Biologia Celular, Universidade Federal do Paraná, CEP 81.531-980, Curitiba, PR, Brazil
[b] Departamento de Física, Universidade Tecnológica Federal do Paraná, DAFIS, CEP 80.230-901, Curitiba, PR, Brazil
[c] Universidade Estadual de Ponta Grossa, Programa Associado de Pós-Graduação em Química, Setor de Ciências Exatas e Naturais, CEP 84.030-900 Ponta Grossa, PR, Brazil
[d] Department of Physics, Chemistry and Pharmacy, University of Southern Denmark, Campusvej 55, DK-5230 Odense M, Denmark
[e] Protein Research Group, Department of Biochemistry and Molecular Biology, University of Southern Denmark, Odense, Denmark

ARTICLE INFO

Article history:
Received 28 August 2016
Received in revised form 2 January 2017
Accepted 3 January 2017
Available online 05 January 2017

Keywords:
HepG2
Silver nanoparticles
Mercury
Cadmium
Co-exposure
Interaction

ABSTRACT

Toxicological interaction represents a challenge to toxicology, particularly for novel contaminants. There are no data whether silver nanoparticles (AgNPs), present in a wide variety of products, can interact and modulate the toxicity of ubiquitous contaminants, such as nonessential metals. In the current study, we investigated the toxicological interactions of AgNP (size = 1–2 nm; zeta potential = −23 mV), cadmium and mercury in human hepatoma HepG2 cells. The results indicated that the co-exposures led to toxicological interactions, with AgNP + Cd being more toxic than AgNP + Hg. Early (2–4 h) increases of ROS (DCF assay) and mitochondrial $O_2^{\bullet -}$ levels (Mitosox® assay) were observed in the cells co-exposed to AgNP + Cd/Hg, in comparison to control and individual contaminants, but the effect was partially reverted in AgNP + Hg at the end of 24 h-exposure. In addition, decreases of mitochondrial metabolism (MTT), cell viability (neutral red uptake assay), cell proliferation (crystal violet assay) and ABC-transporters activity (rhodamine accumulation assay) were also more pronounced in the co-exposure groups. Foremost, co-exposure to AgNP and metals potentiated cell death (mainly by necrosis) and Hg^{2+} (but not Cd^{2+}) intracellular levels (ICP-MS). Therefore, toxicological interactions seem to increase the toxicity of AgNP, cadmium and mercury.

1. Introduction

Silver nanoparticles (AgNP) are present in about 24% of all products listed in the Woodrow Wilson Database (Vance et al., 2015), such as food products, fabrics, cosmetics and medical devices (Seltenrich, 2013; Gaillet and Rouanet, 2015). Due to the extensive production and applications of AgNP, increased amounts of nanowaste will be generated and released into the environment (Bystrzejewska-Piotrowska et al., 2009; Cleveland et al., 2012). It has been already estimated that the predicted environment concentrations (PEC) of AgNP in surface waters is 0.088–10,000 ng l^{-1} and the maximum estimated PEC in wastewater treatment plant effluent is 17 μg l^{-1} (Kim et al., 2015; Maurer-Jones et al., 2013), representing a potential danger to the biota and human health. AgNP can cause adverse effects on a variety of biological models (Morones et al., 2005; Wu et al., 2010; Gliga et al., 2014; Monfared et al., 2015). However, it is not clear whether they represent a threat to the health of vertebrates (Fabrega et al., 2011; Della Torre et al., 2015), particularly when the interactions of AgNP and other environmental contaminants are considered. For example, AgNP, cadmium and mercury can disrupt cell antioxidant defense and induce the production of ROS, DNA damage, apoptosis and promote cell proliferation (Aguado et al., 2013; Chen et al., 2014; Vergilio et al., 2014; Lee et al., 2014; Kim et al., 2015; Kumar et al., 2015), but the effects of the combination of these metals and AgNP are unknown.

Cadmium and mercury are non-essential metals and ubiquitous contaminants of natural environments and dietary products (Monroe and Halvorsen, 2009; Guo et al., 2013; Arbuckle et al., 2016). These metals enter the environment through different anthropogenic sources. Cadmium is used in battery production, fertilizers, paints and plastic stabilizers (Capaldo et al., 2016) and mercury applications include soda chlorine production, coal combustion, paints and seed treatment (Sahu et al., 2014; Syversen and Kaur, 2012). Some studies reported

* Corresponding authors at: Universidade Federal do Paraná, Departamento de Biologia Celular, PO Box: 19031, 81531-980 Curitiba, PR, Brazil.
E-mail addresses: renatam.bio@gmail.com (R.R. Miranda), filipak@ufpr.br (F. Filipak Neto).
[1] The authors contributed equally to this paper and are corresponding authors.

http://dx.doi.org/10.1016/j.tiv.2017.01.003
0887-2333/

that nanoparticles can modulate the toxicity of environmental contaminants, such as metals, polycyclic aromatic hydrocarbons (PAH) and organochlorinated pesticides (OCP), leading to unexpected results (Guo et al., 2013; Ferreira et al., 2014; Kim et al., 2015; Glinski et al., 2016). Guo et al. (2013), for instance, observed positive synergetic interaction of SiNP + $CdCl_2$ for hepatic biochemical and histopathological parameters, as well as the distribution of $CdCl_2$ in the liver and kidneys of mice. Likewise, Kim et al. (2015) reported that co-exposure with citrate coated-AgNP increased the bioaccumulation of Cd in *Daphnia magna*.

Considering the increasing use of AgNP, the widespread metal contamination and therefore, the possibility of these contaminants coexist in natural environments, we investigated the biological effects of combination of AgNP, Cd and Hg in human hepatoma (HepG2) cells through viability, metabolism, proliferation, efflux transporters activity, reactive oxygen species production and cell death parameters, to answer whether the co-exposure increase toxicity. HepG2 cells were selected, since liver is an important target organ of the three contaminants (Fowler, 2009; Stacchiotti et al., 2009; Elsaesser and Howard, 2012). Also, this cell line has been routinely used to investigate the toxicity of several compounds, because it preserves most of the phenotypic characteristics of normal hepatocytes (Knasmüller et al., 2004; Mersch-Sundermann et al., 2004; Urani et al., 2005).

2. Materials and methods

2.1. Silver nanoparticles synthesis and characterization

We synthesized silver nanoparticles through laser ablation in liquid medium (water as solvent) and determined the concentration of the stock solution through flame absorption spectrometry. Shape, diameter, size distribution, zeta potential and spectral properties of AgNP were determined by electron transmission microscopy JEOL 1200 EXII, *Zeta-sizer* (MALVERN®), Dynamic light scattering (DLS) and UV-vis, respectively.

2.2. HepG2 cell culture

Human hepatoma cells HepG2 (Rio de Janeiro Cell bank - Brazil) were cultured as a monolayer in high glucose DMEM medium supplemented with 10% inactivated fetal bovine serum (FBS) and antibiotics (10 U ml^{-1} penicillin and 10 μg/ml streptomycin), at 37 °C and 5% CO_2. Cells at passages 100–110 were utilized in the current study.

2.3. Selection of the concentrations of AgNP, Hg and Cd

Initially, toxicity-screening tests (MTT metabolism and neutral red uptake) were performed, in different concentrations and periods of exposure, for AgNP (0.005–6.66 μg/ml), Hg^{2+} (20–640 μM) and Cd^{2+} (0.5–50 μM) to determine two test concentrations of each contaminant: one that did not induce toxicity and one that induced pronounced toxicity. Based on these results, two concentrations for each contaminant at 24 h time-point were selected (Table 1; data of screenings are not shown).

2.4. Contaminants preparation and exposure protocol

AgNP were synthesized in H_2O and both metals ions stock solutions were prepared in 0.01 M HCl to avoid adsorption to the glass. For the exposure, the contaminants were added to fresh culture medium. In the case of co-exposures, first one contaminant was added to the medium, mixed and then the other contaminant was added. At final, all groups (control, AgNP, metal ions and mixtures) have the same concentration of HCl (buffered by culture medium) and water. Metal ions concentrations are expressed in μM and AgNP concentration is expressed in μg/ml.

Cells were seeded onto 96-well microplate (2×10^5 cells $well^{-1}$) for cytotoxicity, proliferation, reactive oxygen species production and multidrug efflux transporters assays, and onto 6-well plates (1.2×10^6 cells $well^{-1}$) for metal uptake assays. After 24 h, the medium was replaced by fresh DMEM medium with antibiotics and 2% fetal bovine serum containing AgNP ((I) 0.35 μg/ml; (II) 3.5 μg/ml), $CdCl_2$ ((I) 0.15 μM; (II) 1.5 μM) and $HgCl_2$ ((I) 2.8 μM; (II) 28 μM) or the combination of AgNP and each metal. Cells were exposed to these contaminants for 4 and 24 h, and an appropriate control group was kept in parallel. 'I' and 'II' stand, respectively, for the lowest and highest concentrations of AgNP and metals.

Table 1
Experimental design used in the evaluation of the toxicity of AgNP, metals and its association in HepG2 cells.

Groups	Concentration
Control	–
AgNP (I)	0.35 μg/ml
AgNP (II)	3.5 μg/ml
$CdCl_2$ (I)	0.15 μM
$CdCl_2$ (II)	1.5 μM
$HgCl_2$ (I)	2.8 μM
$HgCl_2$ (II)	28 μM
AgNP (I) + $CdCl_2$ (I)	0.35 μg/ml + 0.15 μM
AgNP (I) + $CdCl_2$ (II)	0.35 μg/ml + 1.5 μM
AgNP (II) + $CdCl_2$ (I)	3.5 μg/ml + 0.15 μM
AgNP (II) + $CdCl_2$ (II)	3.5 μg/ml + 1.5 μM
AgNP (I) + HgC_{l2} (I)	0.35 μg/ml + 2.8 μM
AgNP (I) + $HgCl_2$ (II)	0.35 μg/ml + 28 μM
AgNP (II) + $HgCl_2$ (I)	3.5 μg/ml + 2.8 μM
AgNP (II) + $HgCl_2$ (II)	3.5 μg/ml + 28 μM

2.5. Cytotoxicity and proliferation assays

Neutral red (NR) uptake assay was determined after incubation of cells with 50 μg/ml of neutral red for 3 h. MTT assay was determined after incubation of cells with 0.5 mg 1^{-1} of MTT (3-(4,5-dimethylthiazol-2-yl)-2,5-diphenyltetrazolium bromide) for 2 h.

Cell proliferation was determined after DNA staining with 50 μl $well^{-1}$ of 0.25 mg ml^{-1} of violet crystal solution, according to previously published protocols for HepG2 cells (Liebel et al., 2015).

2.6. Reactive oxygen species (ROS) levels

Intracellular ROS levels were evaluated with H_2DCF-DA (2′, 7′-dichlorodihydro-fluorescein diacetate) and MitoSOX™ Red (Invitrogen). After exposure, cells were incubated with either 10 μM of H_2DCF-DA or 5 μM of MitoSOX™, in fresh culture medium, (15 min, 37 °C, protected from light), washed with PBS and suspended in 250 μl of PBS. Fluorescence was measured at 488/530 nm (H_2DCF-DA) and 514/580 nm (MitoSOX; Benov et al., 1998).

2.7. Multidrug efflux transporters activity

The activity of ABC transporters was determined by Rhodamine 123 efflux assay (Pessatti et al., 2002, with modifications for cell culture). Culture medium was replaced by 200 μl of PBS containing 1 μM of rhodamine B, and cells were incubated. Cells were incubated (30 min, 37 °C, protected from light), washed twice with PBS and frozen at −76 °C in 250 μl $well^{-1}$ of PBS. Then, cells were thawed and 200 μl of the lysate were transferred to a black microplate for fluorescence quantification (540/580 nm). Verapamil (20 μM) was utilized as a positive control.

2.8. Cell death

Apoptotic and necrotic cells were detected using the FITC-Annexin V/propidium iodide (PI) Apoptosis Detection Kit (BD Biosciences, Heidelberg, Germany) and analyzed by time-lapse confocal microscopy (during 0–24 h exposure), according to the manufacturer's instructions.

2.9. Intracellular metals concentration

Intracellular content of metals were quantified by inductively coupled plasma mass spectrometry - ICP-MS (Bruker 820-MS + SPS 3 autosampler) (for Ag and Cd) and FIMS (Perkin Elmer FIMS 400 + S 10 autosampler) (for Hg). Cells were seeded onto 6-well plates (1.2×10^6 cells well^{-1}), cultured for 24 h and exposed to the highest concentrations of Hg, Cd, AgNP and their association for 4 h. After exposure, cells were washed 3 times with PBS (to remove AgNP and metals from cell's surface), trypsinized (0.25% trypsin, 0.02% EDTA in PBS, pH 7.2), harvested to tubes with 5 ml culture medium, pelleted (500*g* for 5 min) and suspended in 1 ml culture medium for cell counting. Tubes received 200 μl HNO_3 and 100 μl H_2O_2 (both ICP-MS grade), and remained at −20 °C until the analysis by ICP-MS and FIMS. Metals were quantified in the cells' pellets, exposure culture media and PBS washes. HCl was added to all samples to remove excess H_2O_2, and the samples were left to react overnight. The following morning all samples were diluted and divided into two subsamples, which were then analyzed on either the ICP-MS or the FIMS. Five-point calibration curves were used for quantification, and NIST 1486 (for the ICP-MS) and NIST 1515 (for the FIMS) were used for quality control. Three independent replicates were carried out, and the results are expressed in ppm/10^6 cells.

2.10. Statistical procedures

Three independent experiments were performed. A total of 12 replicates per experiment were utilized for biomarkers analyzed in 96-well microplates. Data distribution was tested and parametric (one-way ANOVA) or nonparametric (Kruskal-Wallis) tests were performed, followed by Dunnett's or Dunn's post-tests (when appropriate). Effects of contaminants were verified by the comparison of the control vs AgNP I and II, Cd I and II, Hg I and II, the four mixtures of AgNP + Cd, or the four mixtures of AgNP + Hg. Toxicological interactions were verified by the comparison of each co-exposure group vs the contaminants alone present in it. Thus, there is only one variable in the statistical comparisons, i.e., the absence/presence of a certain ion/particle. Therefore, it was possible to verify, whether AgNP + Cd/Hg was different from Cd/Hg (variable = presence of AgNP) and AgNP + Cd/Hg was different from AgNP (variable = presence of Cd/Hg). P-values lower than 0.05 were considered statistically significant.

3. Results

3.1. AgNP characterization

Silver nanoparticles, synthesized by laser ablation, had spherical shape, diameter of 1–2 nm (Fig. 1A and B), zeta potential of −23 mV (Zeta-sizer analysis, data not shown) and absorption peak at 400 nm (Fig. 1C).

3.2. Cytotoxicity/viability

The mitochondrial dehydrogenases activity, measured by MTT assay, decreased >20% in cells exposed to the highest AgNP concentration (AgNP II) and the mixtures AgNP II + Hg I/II and AgNP II + Cd I/II for 4 h-experiment (Fig. 2A and B). Decrease of mitochondrial metabolism also occurred in the cells exposed to Cd II (30%), 3 groups of AgNP + Cd and AgNP + Hg II (30%) for 24 h-experiment (Fig. 2C and D). For AgNP II + Cd II (decrease of 60%) and AgNP II + Hg II, the effects were more pronounced than those of individual contaminants (# symbol).

Endosome-lysosome system stability, measured by neutral red assay, decreased after exposure to AgNP II (30%) and Cd II (15%), as well as in the majority of groups containing the association of AgNP + Cd and AgNP + Hg for 4 h-experiment (Fig. 3A and B). However, the effects occurred because of the association of AgNP and metals only for AgNP II + Cd II (50%) and AgNP II + Hg I/II (≈40%; Fig. 3A and B). At 24 h-experiment, neutral red uptake decreased after the exposure to AgNP II and Cd II (25–45%), but not Hg, with effects due to the association only for AgNP II + Cd II (decrease of 80%; Fig. 3C and D). Interestingly, an increase of 20% of NR uptake was observed for Hg I and AgNP I + Hg II (Fig. 3D).

3.3. Cell proliferation

The effect of AgNP and its association with Cd and Hg on cell proliferation was investigated by the crystal violet assay, a cationic dye for DNA. After 24 h, groups exposed to Cd I and Hg I had a slight (10%)

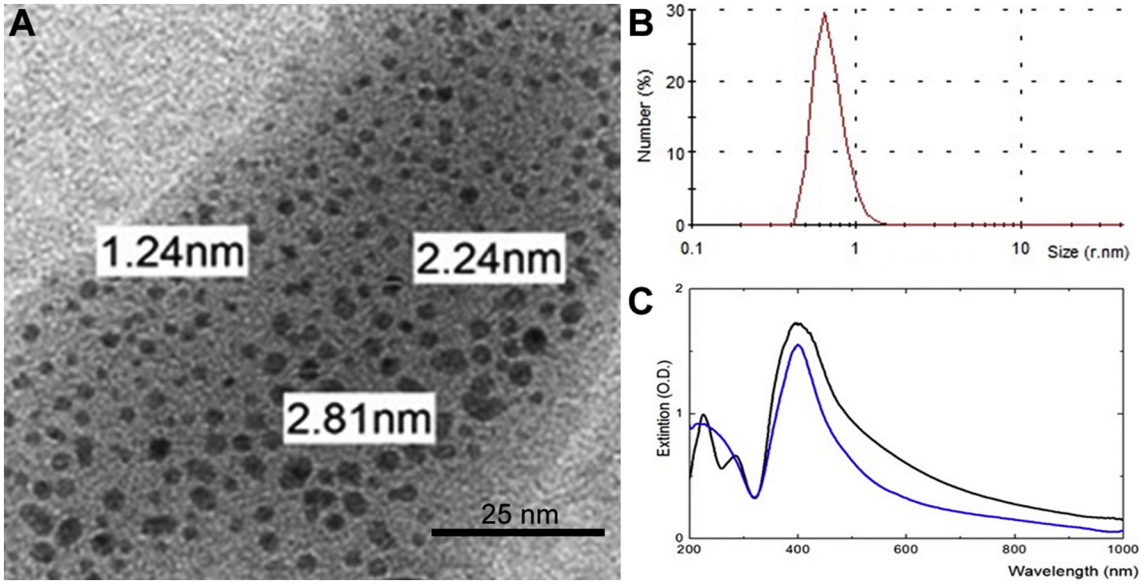

Fig. 1. AgNP characterization. A) TEM image of AgNP suspension. B) Particle distribution according to size (Zeta sizer). C) UV–vis analysis of two AgNP suspensions indicating light peak absorption at 400 nm.

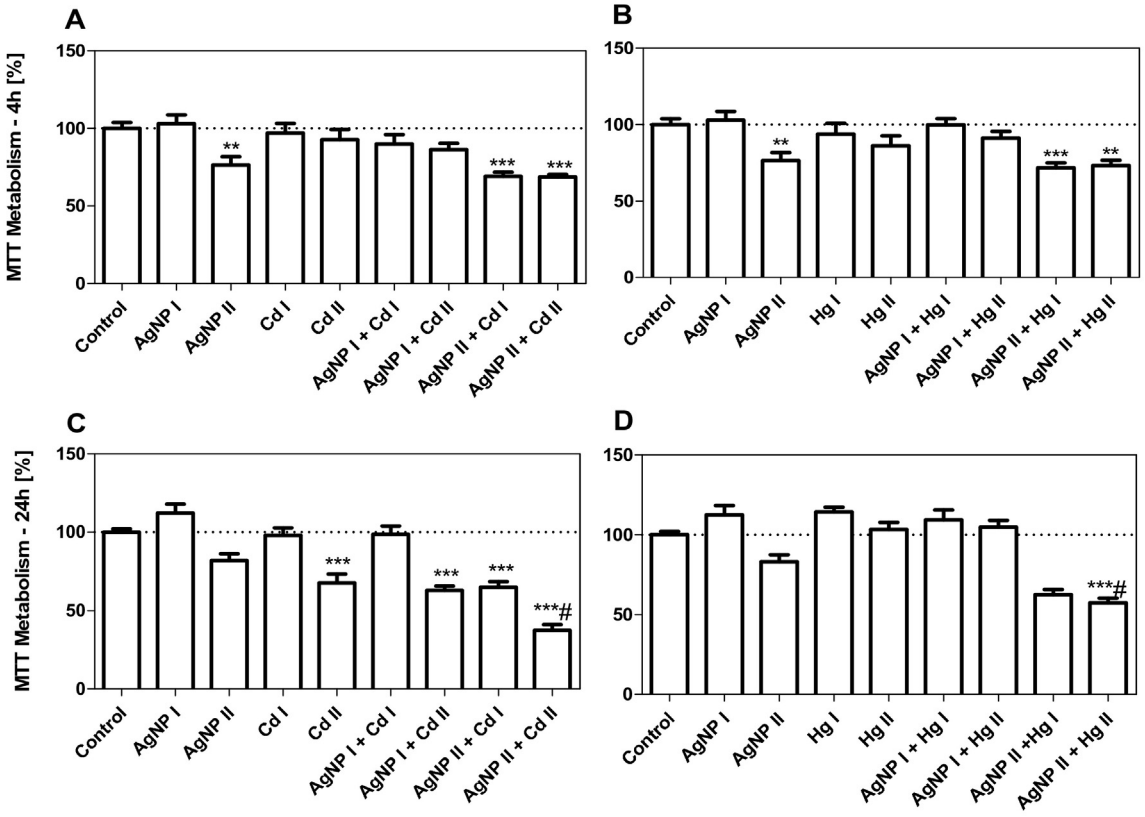

Fig. 2. MTT assay in HepG2 cells exposed for 4 h (A–B) and 24 h (C–D). Values in % compared to control group. Data are presented as the mean + SEM of three independent experiments. Asterisks indicate effects in comparison to control (**$p < 0.01$, ***$p < 0.001$); sharp symbol (#) indicates toxicological interaction.

increase of cell proliferation. However, co-exposure to AgNP II + Cd II and AgNP II + Hg II led to decreases of cell proliferation (40% and 20%, respectively), which were not observed in the cells exposed to the individual contaminants (Fig. 4A and B).

3.4. ROS production

The DCFH-DA probe detected increases of >30% of ROS in the cytoplasm of almost all co-exposed groups short after exposure (at 2 h-experiment), while the individual contaminants did not affect ROS production compared to control (Fig. 5A and B). At 4 h-experiment, ROS concentration increased in the AgNP II group (40%) and, foremost, in the AgNP I/II + Cd II (40–100%) and AgNP II + Hg I/II (70%) groups (Fig. 5C and D). At 24 h-experiment, all the individual contaminants, except for Hg I, induced ROS increases (25–60%). However, only AgNP II + Cd II caused increase of ROS (110%) (Fig. 5E). Co-exposure of AgNP and Hg II for 24 h led to decreases of ROS levels (5% vs control; >20% vs individual contaminants; Fig. 5F).

3.5. Mitochondrial superoxide production

The role of mitochondria in free radical production was also investigated in HepG2 cells. At 4 h-experiment, increases of $O_2^{\bullet -}$ production were observed for AgNP II (95%), Cd II (45%), AgNP II + Cd II (195%) and AgNP II + Hg I/II (50–105%) groups, but not for Hg I/II groups (Fig. 6A and B). For AgNP II + Cd II, the effect can be attributed to the association of contaminants (Fig. 6A). For 24 h-experiment, the contaminants alone did not cause increase of superoxide, except for AgNP II (100% increase). Nevertheless, the co-exposure of AgNP II + Cd II led to 970% increase of $O_2^{\bullet -}$ production (Fig. 6C). Like for 4 h-experiment, some mixtures of AgNP + Cd and AgNP + Hg led to levels of $O_2^{\bullet -}$ different from that of the control, but those effects were not caused by toxicological interaction of the contaminants (Fig. 6C and D; groups have asterisks but not sharp symbols).

3.6. Multidrug efflux transporters activity

The activity of the multidrug efflux transporters was evaluated by rhodamine B accumulation assay: the greater the accumulation, the lower the transporters activity. At 4 h-experiment, the exposure to the contaminants in isolation did not affect rhodamine B accumulation in HepG2 cells. However, levels of rhodamine B were higher in cells exposed to AgNP II + Cd I/II (130–150%) and AgNP II + Hg I/II (90%) than those of control (Fig. 7A and B). At 24 h-experiment, rhodamine B accumulation was higher in AgNP II (30%), Cd II (90%), AgNP I + Cd II (105%) and, foremost, AgNP II + Cd II (415%) groups (Fig. 7C). In both experiments, the effect can be attributed to the association of contaminants only for AgNP II + Cd I/II groups. The co-exposure to AgNP and Hg also led to increases of rhodamine B accumulation at 24 h-experiment (25–60%), but they were statistically equal to at least one of the individual contaminants present in the respective association (Fig. 7D) and so do not characterize an effect of interaction.

3.7. Cell death

To verify whether apoptosis and necrosis were associated with early toxicity of AgNP, Cd and Hg, Annexin V/PI staining was performed in HepG2 cells. Time-lapse images in confocal microscopy showed the progression of cell death during 24 h, with the co-exposure to AgNP II + Cd II, but not to AgNP + Hg II, inducing earlier cellular damage than the

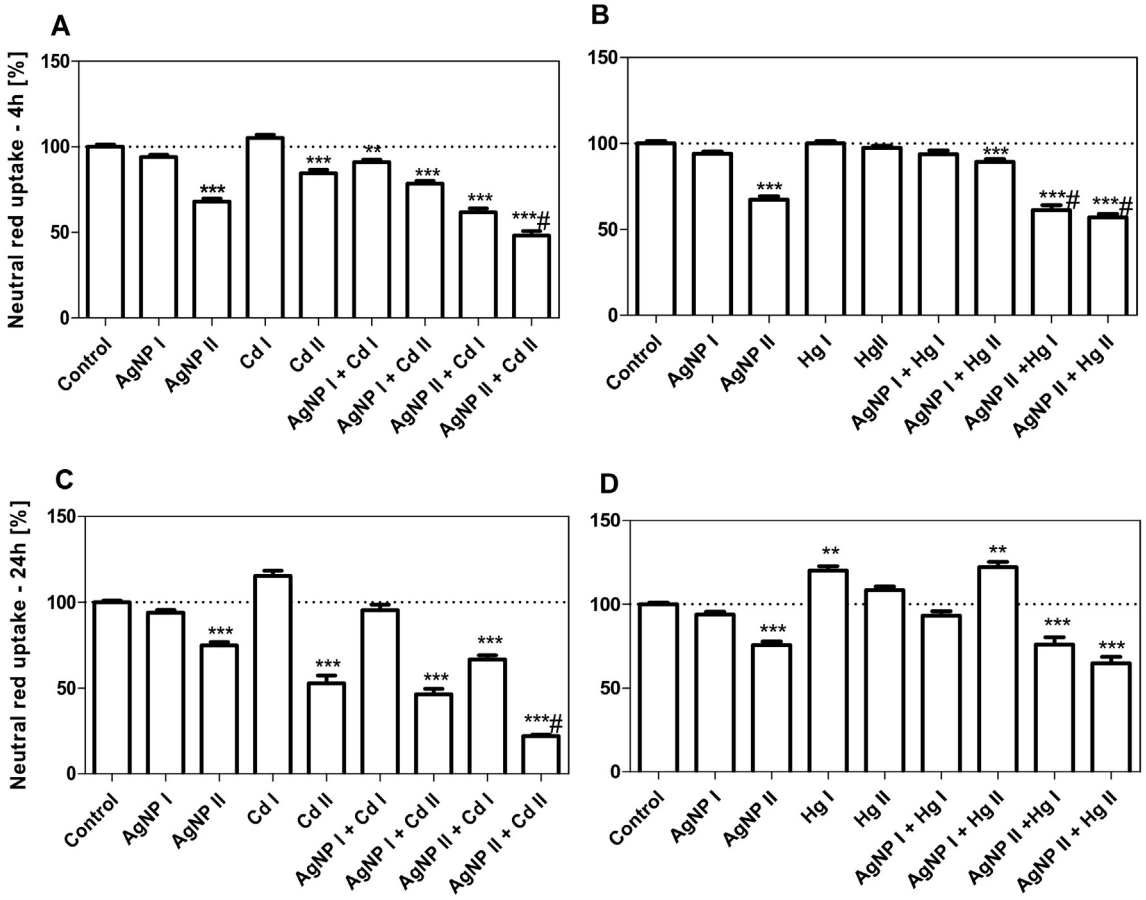

Fig. 3. Neutral red assay in HepG2 cells exposed for 4 h (A–B) and 24 h (C–D). Values in % compared to control group. Data are presented as the mean + SEM of three independent experiments. Asterisks indicate effects in comparison to control (**p < 0.01, ***p < 0.001); sharp symbol (#) indicates toxicological interaction.

individual contaminants (Video in Supplementary material). Interestingly, at the first 12 h, cells seemed to start the apoptotic program, with changes in the cell shape (cells became round), detachment of neighboring cells and decrease of nucleus volume. However, later on, most of the same cells exhibited changes that are characteristic of necrosis. Cells lost the appropriate osmotic balance and swelled up, and plasma membrane became permeable to hydrophilic molecules such as propidium iodide (nucleus that were stained in blue by Hoechst became pink/purple by Hoechst + iodide propidium), with rapid and subsequent phosphatidylserine labeling (in green), and some cells even bursting.

3.8. Intracellular metals concentration

To find whether the higher toxicity observed in cells co-exposed to AgNP and metals was due to higher uptake, intracellular concentrations

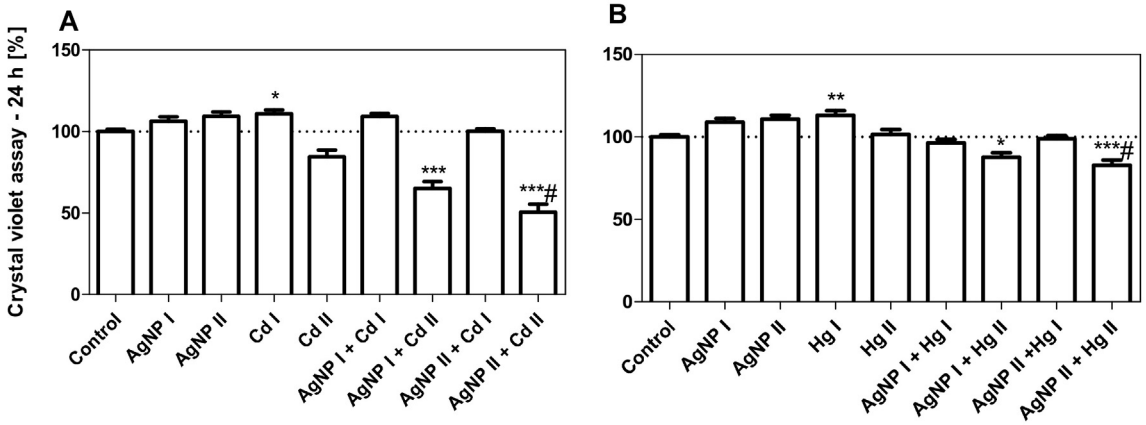

Fig. 4. Cell proliferation assay in HepG2 cells exposed for 24 h. Values in % compared to control group. Data are presented as the mean + SEM of three independent experiments. Asterisks indicate effects in comparison to control (*p < 0.05, **p < 0.01, ***p < 0.001); sharp symbol (#) indicates toxicological interaction.

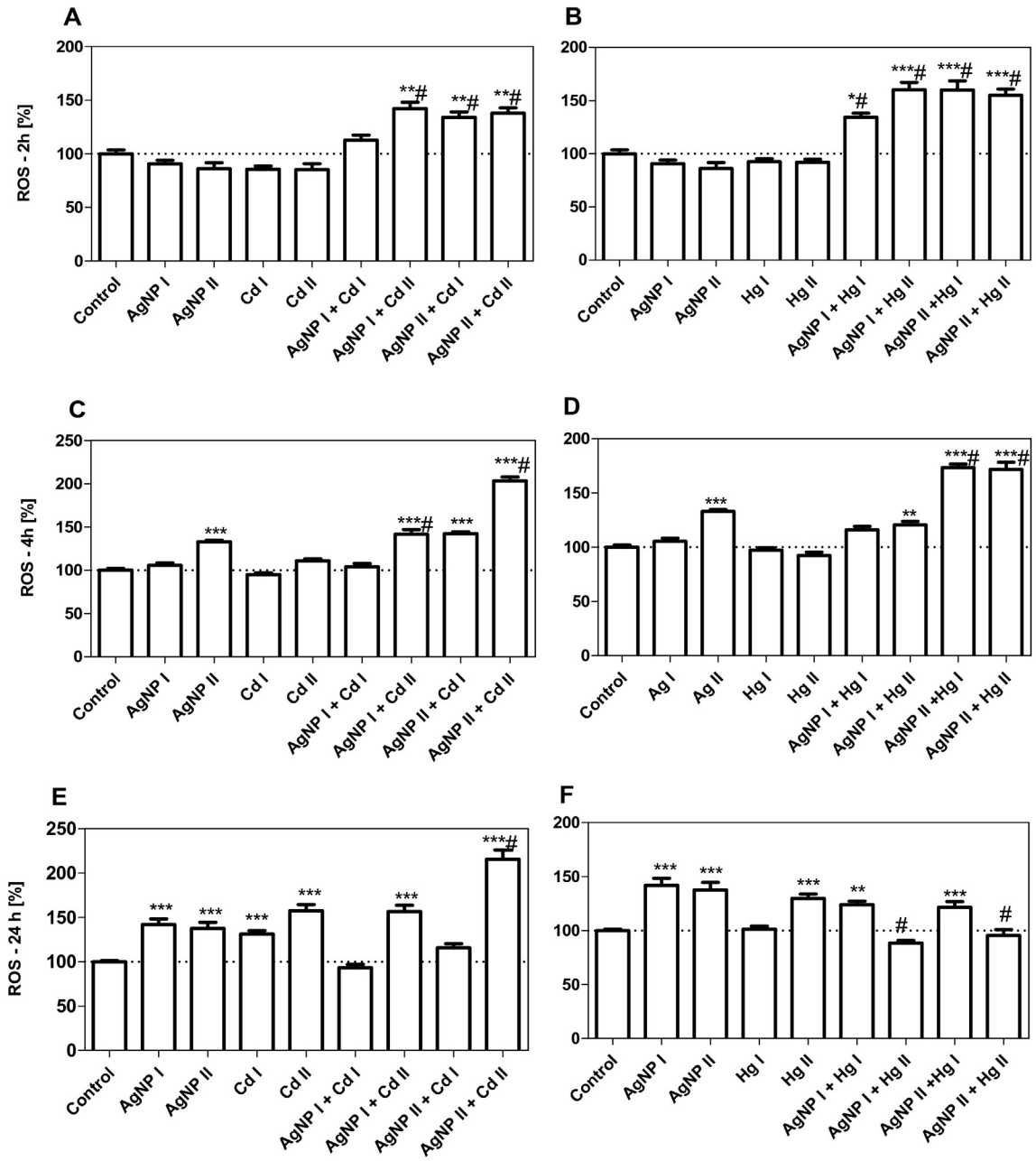

Fig. 5. ROS production relative to cell viability in HepG2 cells after exposure for 2 h (A–B), 4 h (C–D) and 24 h (E–F). Data are presented as the mean + SEM of three independent experiments. Asterisks indicate effects in comparison to control (*p < 0.05, **p < 0.01, ***p < 0.001); sharp symbol (#) indicates toxicological interaction.

of Ag, Cd and Hg were determined by ICP-MS and FIMS, after 4 h of exposure. Co-exposure of AgNP and Cd did not result in a higher uptake of neither the contaminants (Fig. 8A). However, co-exposure of AgNP and Hg resulted in a 2.8-fold increase of Hg concentration in HepG2 cells (Fig. 8B).

4. Discussion

Toxicological interactions occurred in HepG2 cells co-exposed to AgNP + Cd and AgNP + Hg, as follow.

4.1. Contaminants affected cell survivor and the mode of cell death after time-dependent toxicological interaction

The MTT metabolism of cells co-exposed to AgNP II + Hg II for 24 h decreased more than expected, considering the effects of the contaminants alone, while AgNP II + Cd II induced a predicted effect (i.e., similar to the sum of individual contaminants). Both AgNP and Cd can disturb mitochondrial structure and activity of mitochondrial dehydrogenases (responsible for MTT metabolism), leading to ATP depletion (Yano and Marcondes, 2005; Chairuangkitti et al., 2013; Aueviriyavit et al., 2014). This disturb occurred as soon as at 4 h-exposure for AgNP, but not for Cd and Hg, and so AgNP can cause a toxic effect on mitochondria faster than those two toxic metals. Later (24 h), the situation changed as Cd effects on MTT metabolism and cell viability became more pronounced than those of AgNP.

The effect of the association of AgNP + Cd on cell viability varied in a time-dependent manner. At 4 h-exposure, the effect of AgNP II + Cd II was less pronounced than that of 24 h, but induction of lysosomal membrane instability can cause the decrease of neutral red retention observed in both cases, as reported in HepG2 and other cell types (Fotakis and Timbrell, 2006; Messner et al., 2012; Grosse et al., 2013).

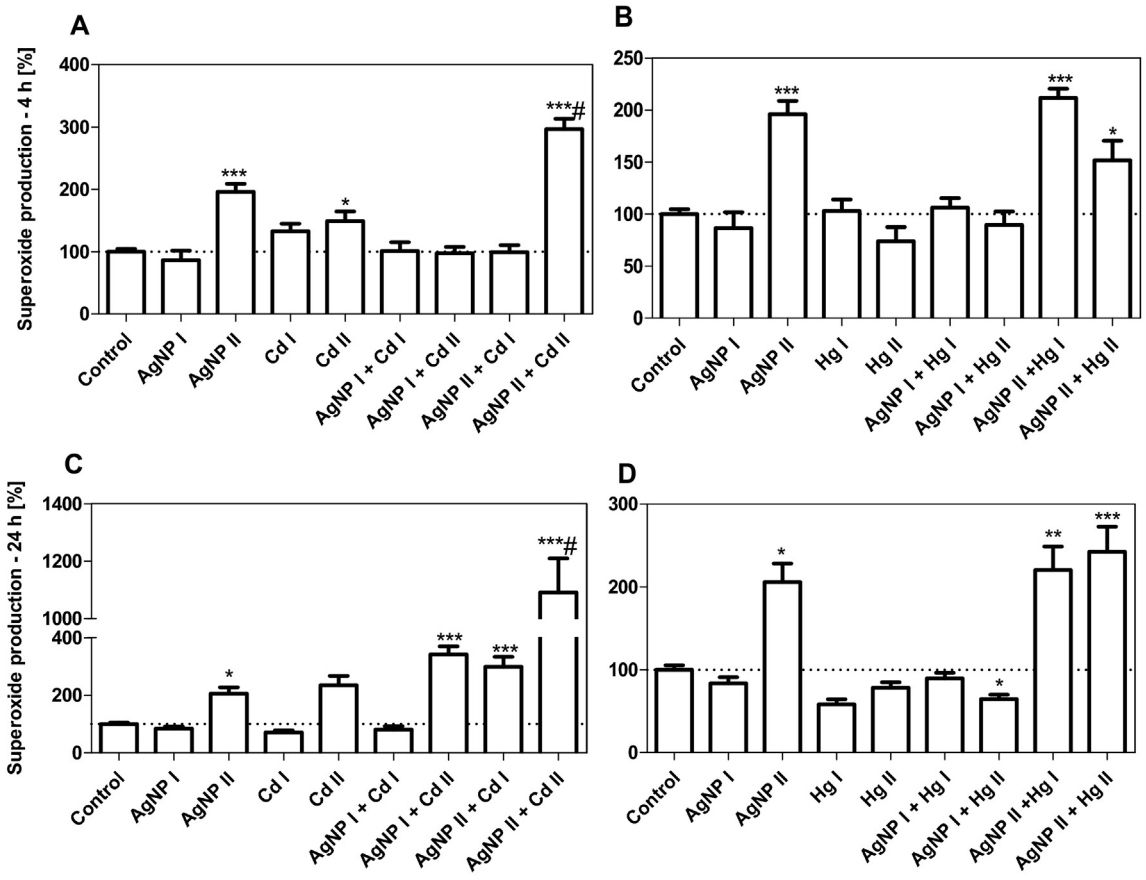

Fig. 6. Superoxide production in mitochondria of HepG2 cells exposed for 4 h (A–B) and 24 h (C–D). Values in % compared to control group. Data are presented as the mean + SEM of three independent experiments. Asterisks indicate effects in comparison to control (*p < 0.05, **p < 0.01, ***p < 0.001); sharp symbol (#) indicates toxicological interaction.

Conversely, a different trend occurred for the AgNP + Hg groups. Hg was not able to impair cell viability after 4 and 24 h-exposure, but the association AgNP II + Hg II reduced it at 4 h, with a partial recovery of neutral red uptake capacity at 24 h. Activation of the defense systems are time-dependent, so that an initial stress can be balanced thereafter, with partial or even overcompensation. The latter situation occurred for Hg I and AgNP I + Hg II groups (decrease of cell viability at 4 h and increased viability/ number of attached cells at 24 h). Else, if defenses are not able to reestablish homeostasis, the toxicity can increase with time, as observed for Cd II. On this regard, though Cd and Hg are both nonessential and electrophilic metals, Cd^{2+} was much more toxic than Hg^{2+} for HepG2 cells.

Co-exposures to the highest concentrations of the contaminants can induce cell death earlier (time-lapse imaging) than the individual contaminants. Cells seem to start apoptosis program with chromatin condensation, but latter plasma membrane usually became permeable to small molecules (e.g., propidium iodide) before phosphatidylserine labeling (with Annexin V-FITC), which is typical for necrosis. Thus, it is possible that chemical stress induced a change of the mode of cell death, from apoptosis to necrosis. Apoptosis requires chemical energy (ATP) which is provided mostly by mitochondria in aerobic eukaryotic cells. AgNP, Cd and Hg can impair mitochondrial membrane potential and ATP synthesis (Monroe and Halvorsen, 2009; Tomankova et al., 2015), leading to ATP depletion and necrosis; necrosis is a passive process and does not require ATP.

Changes in cell proliferation after contaminant exposure depends on many factors, such as time of exposure and concentration. Many studies reported the ability of AgNP and both metal ions (Cd and Hg) to reduce cell proliferation (Templeton and Liu, 2010; Vergilio et al., 2014; Miethling-Graff et al., 2014). In this study, contaminants alone did not impair cell proliferation, though co-exposures seem to induce an inhibitory effect that could not be predicted based on the results from the lone exposures. Decreased metabolic status of the cells (MTT assay) and cell death after exposure to AgNP II + Cd II or to AgNP II + Hg II could explain, at least in part, the decrease of the number of attached cells (determined through crystal violet assay). Conversely, activation of cell defense mechanisms could lead to the increases of cell number observed in the cells exposed to the lowest Cd and Hg concentrations.

4.2. ROS production increased early after the co-exposures

Oxidative stress is one of the hallmarks of AgNP toxicity (Asharani et al., 2008; Kim et al., 2009; Liu et al., 2010). Cadmium and mercury can also induce the increase of ROS levels, by binding to sulfhydryl groups of antioxidants such as glutathione, inhibiting antioxidant enzymes (Nzengue et al., 2008; Aguado et al., 2013) and blocking electron flow in mitochondria (Monroe and Halvorsen, 2009). In the current study, increase of ROS production was an early response (observed from 2 h-experiment on) in cells co-exposed to AgNP and Cd/Hg, but not in cells exposed to the individual contaminants. For longer exposures, individual contaminants were able to unbalance redox milieu, and the effects of the associations became less evident (4 h-experiment) until being only observed in AgNP II + Cd II and AgNP I/II + Hg II groups (24 h-experiment). Thus, cellular defense systems may be efficient to avoid oxidative stress at very short-term exposures, but not at longer-term ones for individual contaminants. For the associations of AgNP and Cd/Hg, defenses were not enough to deal with ROS at 2 h-exposures and avoid cell death during the course of 24 h-exposure.

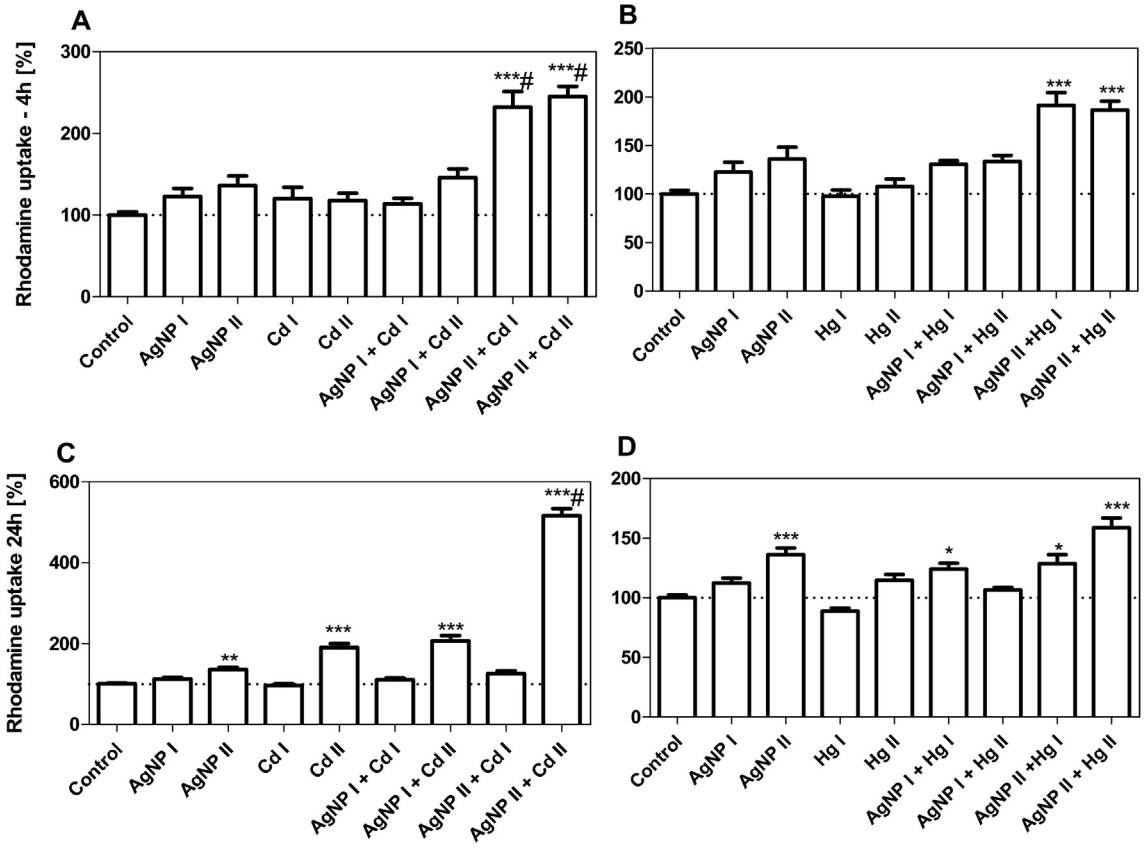

Fig. 7. Rhodamine accumulation assay in HepG2 cells exposed for 4 h (A–B) and 24 h (C–D). Values in % compared to control group. Data are presented as the mean + SEM of three independent experiments. Asterisks indicate effects in comparison to control (*p < 0.05, **p < 0.01, ***p < 0.001); sharp symbol (#) indicates toxicological interaction. The greater the rhodamine accumulation, the lower the activity of the xenobiotic efflux transporters.

Mitochondria were one important source of ROS in the cells exposed to AgNP and Cd, but not Hg, as well as in cells co-exposed to AgNP II + Cd II; for the latter group, superoxide levels increased with the exposure time. Excess of ROS in mitochondria can lead to organelle malfunction (e.g., decreased enzymatic activity and MTT metabolism) and ATP depletion, as well as malfunction or damage to the other cell compartments, as unstable superoxide can be converted to much more stable and membrane-permeable hydrogen peroxide (Fleury et al., 2002). Decrease of ATP levels can, in turn, impair active transport processes such as proton transport into endosomes and lysosomes (decreasing neutral red retention) and rhodamine transport out the cell (by ABC efflux transporters), as well as impair the execution of apoptosis program.

4.3. Rhodamine accumulation followed the same pattern of mitochondrial ROS levels

ABC transporters are a superfamily of membrane transporters that use energy from ATP hydrolysis to translocate a broad-spectrum of

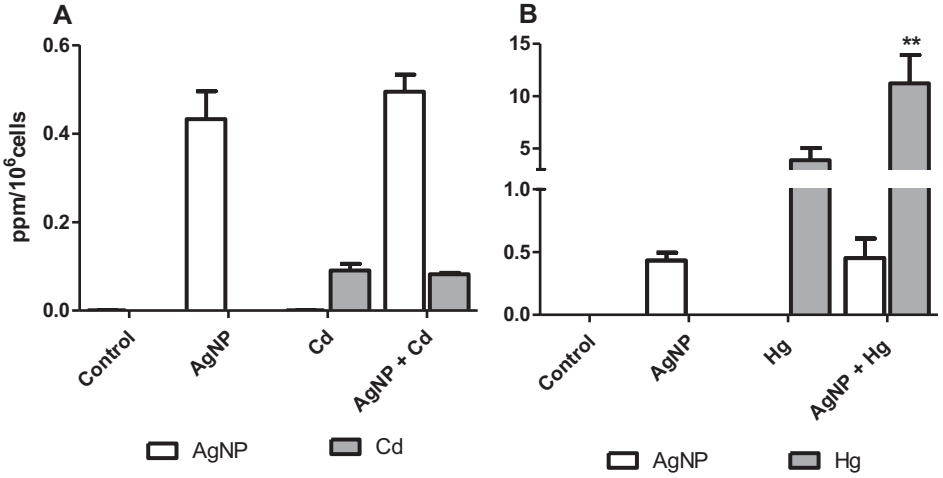

Fig. 8. Intracellular concentration of Ag, Cd and Hg in HepG2 cells exposed for 4 h (A–B). Results are expressed in ppm/10^6 cells. Data are presented as the mean + SEM of three independent experiments. **p < 0.01.

molecules across cell membranes (Rodrigues et al., 2009). One of these transporters, P-glycoprotein (P-gp), is involved with the transport of cell lipids and drugs (Klein et al., 1999), being important for cell detoxification. In HepG2 cells, accumulation of rhodamine B, associated with the malfunction of the efflux system, occurred in all AgNP II-containing associations (AgNP II + Cd I/II; AgNP II + Hg I/II) as early as at 4 h-experiment, with no effect on the individual exposures. However, as observed for mitochondrial ROS levels, even individual contaminants affected rhodamine B accumulation after 24 h-exposure. Regardless of the exact cause of efflux transporters impairment, i.e. decrease of ATP levels or direct damage to the transporters (by metals or ROS), cells may become more sensitive to additional chemical stressors that are substrates for the transporters, as they might remain longer inside the cells.

4.4. Higher accumulation of the metal can explain the higher toxicity of the association containing Hg, but not Cd

Metals such as Cd and Pb can adsorb onto AgNP surface due to the nanoparticle's highly reactive surface and charge difference (Alqudami et al., 2012). Since AgNP used in the experiments exhibit negative charge, as showed by zeta potential, and both Cd and Hg ions are positively charged, it is possible that AgNP absorbed these ions.

ICP-MS analysis were performed in order to find if the increase of toxicity, observed in co-exposed cells, was the outcome of a higher intracellular concentration of one or both contaminants. In the presence of AgNP, concentration of Hg ions increased about 2.8 fold in HepG2 cells after 4 h-exposure. This might explain the increased toxic effect of AgNP + Hg groups in some parameters, such as cell metabolism, viability, and proliferation, as well as ROS production. However, this logic is not valid for Cd ions, since the presence of AgNP did not affect intracellular Cd ions concentration, but co-exposures AgNP + Cd were much more toxic. For AgNP + Cd, each contaminant may independently interfere with converting toxic pathways (e.g., mitochondrial ATP synthesis) resulting in a toxicological interaction. An alternative hypothesis, that needs investigation, is that the interaction was only a consequence of the fact that a cell under some level of stress (by a contaminant) may be able to deal with it but not with additional stress (by the other contaminant) because the sum of both stresses exceeds cells defenses, independent of the nature of the contaminants.

5. Final comments

Taken together, these results provide important information about the toxicological interaction of AgNP, cadmium and mercury in HepG2 cells. Associations of AgNP and the metal ions were more toxic than the individual contaminants. Expected effects were observed in most co-exposures, whereas in few cases the effects of the mixtures were higher than the sum of the effects observed for the individual contaminants. ROS production was an early effect of the co-exposures, with important contribution of mitochondria. Decrease of mitochondrial metabolism and ATP levels can, in principle, explain the other findings in HepG2 cells: the accumulation of rhodamine B (decreased efflux transporters activity), decreased viability (decreased neutral red retention) and change of the mode of cell death (apoptosis to necrosis). Highest intracellular concentration of Hg in the presence of AgNP can explain the highest toxicity of AgNP + Hg association. For AgNP + Cd groups, AgNP had no effect on Cd uptake.

Supplementary data to this article can be found online at http://dx.doi.org/10.1016/j.tiv.2017.01.003.

Conflict of interest statement

The authors declare that there are no conflicts of interest.

Transparency document

The Transparency document associated with this article can be found, in online version.

Acknowledgements

CNPq (Grant number 480707/2013-8), (Brazilian Agency for Science and Technology) and CAPES (PhD scholarship) supported the work described in the current paper. The authors thank Israel Henrique Bini for the assistance with the confocal microscope. The authors also gratefully acknowledge financial support by the European Research Council (ERC) under the European Union's Horizon 2020 Research and Innovation Programme (grant agreement No. 646603) as well the VILLUM Center for Bioanalytical Sciences at the University of Southern Denmark.

References

Aguado, A., Galán, M., Zhenyukh, O., Wiggers, G.A., Roque, F.R., Redondo, S., Peçanha, F., Martín, A., Fortuño, A., Cachofeiro, V., Tejerina, T., Salaices, M., Briones, A.M., 2013. Mercury induces proliferation and reduces cell size in vascular smooth muscle cells through MAPK, oxidative stress and cyclooxygenase-2 pathways. Toxicol Appl. Pharmacol. 268 (2), 188–200.

Alqudami, A., Alhemiary, N.a., Munassar, S., 2012. Removal of Pb(II) and Cd(II) ions from water by Fe and Ag nanoparticles prepared using electro-exploding wire technique. Environ. Sci. Pollut. Res. 19, 2832–2841.

Arbuckle, T.E., Liang, C.L., Morisset, A.-S., Fisher, M., Weiler, H., Cirtiu, C.M., Legrand, M., Davis, K., Ettinger, A.S., Fraser, W.D., 2016. Maternal and fetal exposure to cadmium, lead, manganese and mercury: the MIREC study. Chemosphere 163, 270–282.

Asharani, P.V., Wu, Y.L., Gong, Z., Valiyaveettil, S., 2008. Toxicity of Silver Nanoparticles in Zebrafish Models. p. 255102.

Aueviriyavit, S., Phummiratch, D., Maniratanachote, R., 2014. Mechanistic study on the biological effects of silver and gold nanoparticles in Caco-2 cells—induction of the Nrf2/HO-1 pathway by high concentrations of silver nanoparticles. Toxicol. Lett. 224, 73–83.

Benov, L., Sztejnberg, L., Fridovich, I., Enov, L.U.B., Ztejnberg, L.A.S., 1998. Critical evaluation of the use of hydroethidine as a measure of superoxide anion radical. Free Radic. Biol. Med. 25, 826–831.

Bystrzejewska-Piotrowska, G., Golimowski, J., Urban, P.L., 2009. Nanoparticles: their potential toxicity, waste and environmental management. Waste Manag. 29, 2587–2595.

Capaldo, A., Gay, F., Scudiero, R., Trinchella, F., Caputo, I., Lepretti, M., Marabotti, A., Esposito, C., Laforgia, V., 2016. Histological changes, apoptosis and metallothionein levels in *Triturus carnifex* (Amphibia, Urodela) exposed to environmental cadmium concentrations. Aquat. Toxicol. 173, 63–73.

Chairuangkitti, P., Lawanprasert, S., Roytrakul, S., Aueviriyavit, S., Phummiratch, D., Kulthong, K., Chanvorachote, P., Maniratanachote, R., 2013. Silver nanoparticles induce toxicity in A549 cells via ROS-dependent and ROS-independent pathways. Toxicol. in Vitro 27, 330–338.

Chen, Y.Y., Zhu, J.Y., Chan, K.M., 2014. Effects of cadmium on cell proliferation, apoptosis, and proto-oncogene expression in zebrafish liver cells. Aquat. Toxicol. 157, 196–206.

Cleveland, D., Long, S.E., Pennington, P.L., Cooper, E., Fulton, M.H., Scott, G.I., Brewer, T., Davis, J., Petersen, E.J., Wood, L., 2012. Pilot estuarine mesocosm study on the environmental fate of silver nanomaterials leached from consumer products. Sci. Total Environ. 421–422, 267–272.

Della Torre, C., Balbi, T., Grassi, G., Frenzilli, G., Bernardeschi, M., Smerilli, A., Guidi, P., Canesi, L., Nigro, M., Monaci, F., Scarcelli, V., Rocco, L., Focardi, S., Monopoli, M., Corsi, I., 2015. Titanium dioxide nanoparticles modulate the toxicological response to cadmium in the gills of *Mytilus galloprovincialis*. J. Hazard. Mater. 297, 92–100.

Elsaesser, A., Howard, C.V., 2012. Toxicology of nanoparticles. Adv. Drug Deliv. Rev. 64, 129–137.

Fabrega, J., Luoma, S.N., Tyler, C.R., Galloway, T.S., Lead, J.R., 2011. Silver nanoparticles: behaviour and effects in the aquatic environment. Environ. Int. 37, 517–531.

Ferreira, J.L.R., Lonné, M.N., França, T.A., Maximilla, N.R., Lugokenski, T.H., Costa, P.G., Fillmann, G., Antunes Soares, F.A., de la Torre, F.R., Monserrat, J.M., 2014. Co-exposure of the organic nanomaterial fullerene C60 with benzo[a]pyrene in *Danio rerio* (zebrafish) hepatocytes: evidence of toxicological interactions. Aquat. Toxicol. 147, 76–83.

Fleury, C., Mignotte, B., Vayssière, J.-L., 2002. Mitochondrial reactive oxygen species in cell death signaling. Biochimie 84, 131–141.

Fotakis, G., Timbrell, J.A., 2006. Role of trace elements in cadmium chloride uptake in hepatoma cell lines. Toxicol. Lett. 164, 97–103.

Fowler, B.A., 2009. Monitoring of human populations for early markers of cadmium toxicity: a review. Toxicol. Appl. Pharmacol. 238, 294–300.

Gaillet, S., Rouanet, J.-M., 2015. Silver nanoparticles: their potential toxic effects after oral exposure and underlying mechanisms—a review. Food Chem. Toxicol. 77, 58–63.

Gliga, A.R., Skoglund, S., Wallinder, I.O., Fadeel, B., Karlsson, H.L., 2014. Size-dependent cytotoxicity of silver nanoparticles in human lung cells: the role of cellular uptake, agglomeration and Ag release. Part. Fibre Toxicol. 11, 11.

Glinski, A., Liebel, S., Pelletier, È., Voigt, C.L., Randi, M.A.F., Campos, S.X., Oliveira Ribeiro, C.A., Filipak Neto, F., 2016. Toxicological interactions of silver nanoparticles and

organochlorine pesticides in mouse peritoneal macrophages. Toxicol. Mech. Methods 26, 251–259.
Grosse, S., Evje, L., Syversen, T., 2013. Silver nanoparticle-induced cytotoxicity in rat brain endothelial cell culture. Toxicol. in Vitro 27, 305–313.
Guo, M., Xu, X., Yan, X., Wang, S., Gao, S., Zhu, S., 2013. In vivo biodistribution and synergistic toxicity of silica nanoparticles and cadmium chloride in mice. J. Hazard. Mater. 260, 780–788.
Kim, S., Choi, J.E., Choi, J., Chung, K.-H., Park, K., Yi, J., Ryu, D.-Y., 2009. Oxidative stress-dependent toxicity of silver nanoparticles in human hepatoma cells. Toxicol. in Vitro 23, 1076–1084.
Kim, I., Lee, B.-T., Kim, H.-A., Kim, K.-W., Kim, S.D., Hwang, Y.-S., 2015. Citrate coated silver nanoparticles change heavy metal toxicities and bioaccumulation of *Daphnia magna*. Chemosphere 143, 99–105.
Klein, I., Sarkadi, B., Váradi, A., 1999. An inventory of the human ABC proteins. Biochim. Biophys. Acta Biomembr. 1461, 237–262.
Knasmüller, S., Mersch-Sundermann, V., Kevekordes, S., Darroudi, F., Huber, W.W., Hoelzl, C., Bichler, J., Majer, B.J., 2004. Use of human-derived liver cell lines for the detection of environmental and dietary genotoxicants; current state of knowledge. Toxicology 198, 315–328.
Kumar, G., Degheidy, H., Casey, B.J., Goering, P.L., 2015. Flow cytometry evaluation of in vitro cellular necrosis and apoptosis induced by silver nanoparticles. Food Chem. Toxicol. 85, 45–51.
Lee, Y.-H., Cheng, F.-Y., Chiu, H.-W., Tsai, J.-C., Fang, C.-Y., Chen, C.-W., Wang, Y.-J., 2014. Cytotoxicity, oxidative stress, apoptosis and the autophagic effects of silver nanoparticles in mouse embryonic fibroblasts. Biomaterials 35 (16), 4706–4715.
Liebel, S., de Oliveira Ribeiro, C.A., de Magalhães, V.F., da Silva, R.D.C., Rossi, S.C., Randi, M.A.F., Filipak Neto, F., 2015. Low concentrations of cylindrospermopsin induce increases of reactive oxygen species levels, metabolism and proliferation in human hepatoma cells (HepG2). Toxicol. in Vitro 29, 479–488.
Liu, W., Wu, Y., Wang, C., Li, H.C., Wang, T., Liao, C.Y., Cui, L., Zhou, Q.F., Yan, B., Jiang, G.B., 2010. Impact of silver nanoparticles on human cells: effect of particle size. Nanotoxicology 4, 319–330.
Maurer-Jones, M.a., Gunsolus, I.L., Murphy, C.J., Haynes, C.L., 2013. Toxicity of engineered nanoparticles in the environment. Anal. Chem. 85, 3036–3049.
Mersch-Sundermann, V., Knasmüller, S., Wu, X.J., Darroudi, F., Kassie, F., 2004. Use of a human-derived liver cell line for the detection of cytoprotective, antigenotoxic and cogenotoxic agents. Toxicology 198, 329–340.
Messner, B., Ploner, C., Laufer, G., Bernhard, D., 2012. Cadmium activates a programmed, lysosomal membrane permeabilization-dependent necrosis pathway. Toxicol. Lett. 212, 268–275.
Miethling-Graff, R., Rumpker, R., Richter, M., Verano-Braga, T., Kjeldsen, F., Brewer, J., Hoyland, J., Rubahn, H.-G., Erdmann, H., 2014. Exposure to silver nanoparticles induces size- and dose-dependent oxidative stress and cytotoxicity in human colon carcinoma cells. Toxicol. in Vitro 28, 1280–1289.
Monfared, A.L., Bahrami, A.M., Hosseini, E., Soltani, S., Shaddel, M., 2015. Effects of nanoparticles on histo-pathological changes of the fish. J. Environ. Health Sci. Eng. 13, 62.
Monroe, R.K., Halvorsen, S.W., 2009. Environmental toxicants inhibit neuronal Jak tyrosine kinase by mitochondrial disruption. Neurotoxicology 30, 589–598.
Morones, J.R., Elechiguerra, J.L., Camacho, A., Holt, K., Kouri, J.B., Ramírez, J.T., Yacaman, M.J., 2005. The bactericidal effect of silver nanoparticles. Nanotechnology 16, 2346–2353.
Nzengue, Y., Steiman, R., Garrel, C., Lefèbvre, E., Guiraud, P., 2008. Oxidative stress and DNA damage induced by cadmium in the human keratinocyte HaCaT cell line: role of glutathione in the resistance to cadmium. Toxicology 243, 193–206.
Pessatti, M.L., Resgalla Jr., C., Reis, F.R.W., Kuehn, J., Salomão, L.C., Fontana, J.D., 2002. Variability of rates of filtration, respiration and assimilation and multixenobiotic mechanism resistance (MXR) of mussel *Perna perna* under lead influence. Br. J. Biol. 62, 651–656.
Rodrigues, A.C., Curi, R., Hirata, M.H., Hirata, R.D.C., 2009. Decreased ABCB1 mRNA expression induced by atorvastatin results from enhanced mRNA degradation in HepG2 cells. Eur. J. Pharm. Sci. 37, 486–491.
Sahu, S.K., Bhangare, R.C., Tiwari, M., Ajmal, P.Y., Pandit, G.G., 2014. Depth profiles of lithogenic and anthropogenic mercury in the sediments from Thane Creek, Mumbai, India. Int. J. Sediment Res. 29, 131–139.
Seltenrich, N., 2013. Nanosilver: weighing the risks and benefits. Environ. Health Perspect. 121, 220–225.
Stacchiotti, A., Morandini, F., Bettoni, F., Schena, I., Lavazza, A., Giovanni, P., Apostoli, P., Rezzani, R., Francesca, M., 2009. Stress proteins and oxidative damage in a renal derived cell line exposed to inorganic mercury and lead. Toxicology 264, 215–224.
Syversen, T., Kaur, P., 2012. The toxicology of mercury and its compounds. J. Trace Elem. Med. Biol. 26, 115–126.
Templeton, D.M., Liu, Y., 2010. Chemico-biological interactions multiple roles of cadmium in cell death and survival. Chem. Biol. Interact. 188, 267–275.
Tomankova, K., Horakova, J., Harvanova, M., Malina, L., Soukupova, J., Hradilova, S., Kejlova, K., Malohlava, J., Licman, L., Dvorakova, M., Jirova, D., Kolarova, H., 2015. Cytotoxicity, cell uptake and microscopic analysis of titanium dioxide and silver nanoparticles in vitro. Food Chem. Toxicol. 82, 106–115.
Urani, C., Melchioretto, P., Canevali, C., Crosta, G.F., 2005. Cytotoxicity and induction of protective mechanisms in HepG2 cells exposed to cadmium. Toxicol. in Vitro 19, 887–892.
Vance, M.E., Kuiken, T., Vejerano, E.P., McGinnis, S.P., Hochella, M.F., Hull, D.R., 2015. Nanotechnology in the real world: redeveloping the nanomaterial consumer products inventory. Beilstein J. Nanotechnol. 6, 1769–1780.
Vergilio, C.S., Carvalho, C.E.V., Melo, E.J.T., 2014. Mercury-induced dysfunctions in multiple organelles leading to cell death. Toxicol. in Vitro 29, 63–71.
Wu, Y., Zhou, Q., Li, H., Liu, W., Wang, T., Jiang, G., 2010. Effects of silver nanoparticles on the development and histopathology biomarkers of Japanese medaka (*Oryzias latipes*) using the partial-life test. Aquat. Toxicol. 100, 160–167.
Yano, C.L., Marcondes, M.C.C.G., 2005. Cadmium chloride-induced oxidative stress in skeletal muscle cells in vitro. Free Radic. Biol. Med. 39, 1378–1384.